Quasiparticle Excitations and Charge Transition Levels of Oxygen Vacancies in Hafnia

Manish Jain,[1,2] James R. Chelikowsky,[3] and Steven G. Louie[1,2]

[1]*Department of Physics, University of California, Berkeley, California 94720, USA*
[2]*Materials Sciences Division, Lawrence Berkeley, National Laboratory, Berkeley, California 94720, USA*
[3]*Center for Computational Materials, Institute for Computational Engineering and Sciences, Departments of Physics and Chemical Engineering, University of Texas, Austin, Texas 78712, USA*

(Received 5 May 2011; published 16 November 2011)

We calculate the quasiparticle defect states and charge transition levels (CTLs) of oxygen vacancies in monoclinic hafnia using density functional theory (DFT) and the *GW* method. We introduce the criterion that the quality and reliability of CTLs may be evaluated by calculating the same CTL via two physical paths and show that it is necessary to include important electrostatic corrections previously neglected within the supercell DFT + *GW* approach. Contrary to previous reports, the oxygen vacancies in hafnia are large positive *U* centers, where *U* is the defect charging energy.

DOI: 10.1103/PhysRevLett.107.216803 PACS numbers: 73.40.Qv, 61.72.jd, 85.30.Tv

Hafnia has recently received much attention because of its many applications, in particular, as high-dielectric gate material replacing silica in microelectronic devices. However, devices based on hafnia suffer from several problems such as voltage threshold instabilities [1] and flat band voltage shifts [2]. These problems are believed to be due to a high density of defects in the material; in particular, oxygen vacancies are believed to play an important role as electron traps.

There have been several theoretical studies on the structural and electronic properties of oxygen vacancies in monoclinic hafnia. In early studies, formation energies as well as defect levels were calculated within DFT using the local density approximation [3] and the generalized gradient approximation [4]. The defect charging energy, *U*, for adding an electron to the defect was calculated and the vacancies were found to be negative *U* [5] centers within these approximations. In these studies, however, the defect levels in the gap could not be determined unambiguously, owing to the well-known problem of underestimation of band gaps using Kohn-Sham eigenvalues [6]. Later studies used hybrid functionals [7–9]. These functionals, which were constructed to fix the band gap problem, found that the defect has a small positive *U* (~ 0.3 eV) [8]. Recently, there has been a higher level theory study [10] using a combined DFT and *GW* approach on these defects. These authors also found a negative *U* behavior for the oxygen vacancy. The *GW* part of the study in Ref. [10] was, however restricted to a 24-atom supercell.

In this letter, we report a new study of the quasiparticle (QP) excitations and CTLs of oxygen vacancies in monoclinic hafnia using the combined approach [11] based on DFT and *GW* formalism [6]. The DFT + *GW* formalism corrects for the error incurred in calculating formation energy and CTLs within standard DFT. We introduce three novel features into our study not considered in previous work. (i) We computed the CTLs via two physical paths. This procedure provides a means to determine *a priori* when the calculation has achieved an accurate, consistent result which was not possible before. (ii) We demonstrate that it is absolutely necessary to include an theretofore missed electrostatic correction to obtain the true values for the CTLs within the DFT + *GW* approach. (iii) A new partitioning of the defect charging energy into a lattice and QP gap contribution is formulated, which provides insight into their structure and properties.

The oxygen defects in hafnia are found to be large positive *U* centers ($U \sim 1$ eV). Our calculations were done using large supercells with 96 atoms. Such large supercells are necessary to minimize any spurious defect-defect interactions from overlap of the defect-state wave functions in neighboring supercells.

The formation energy of a defect in charge state q and at arbitrary ionic coordinates $\mathbf{R}$ and chemical potential μ, $E_q^f(\mathbf{R})[\mu]$, can be expressed as

$$E_q^f(\mathbf{R})[\mu] = E_q(\mathbf{R}) - E_{\mathrm{ref}} + \mu q, \tag{1}$$

where $E_q(\mathbf{R})$ is the total energy of the system and E_{ref} is the energy of a reference system with the same number of atoms as the charged system. We note that $\mathbf{R}$ is an arbitrary configuration which needs not be the equilibrium configuration of the charge state q which we denote as $\mathbf{R}_q$. The CTL, $\varepsilon^{q/q-1}$, is defined as the value of the chemical potential at which the charge state of the defect changes from q to $q-1$ ($q/q-1$). Conventionally, one measures the CTL from the valence band maximum, E_v. It is defined as the chemical potential μ at which the formation energies of the q and $q-1$ defects are equal and can be written in terms of formation energies as

$$\varepsilon^{q/q-1} = E_{q-1}^f(\mathbf{R}_{q-1})[\mu = E_v] - E_q^f(\mathbf{R}_q)[\mu = E_v]. \tag{2}$$

Within standard DFT, CTL is determined by calculating each of the formation energies in Eq. (2) in their respective equilibrium configurations as accurately as possible. But, because of the band gap problem and self-interaction terms within standard DFT methods, significant errors may be introduced. However, within the combined DFT and *GW* formalism, a CTL can be written as

$$\begin{aligned}\varepsilon^{q/q-1} &= [E^f_{q-1}(\mathbf{R}_{q-1}) - E^f_{q-1}(\mathbf{R}_q)] \\ &\quad + [E^f_{q-1}(\mathbf{R}_q) - E^f_q(\mathbf{R}_q)] \\ &\equiv E_{\text{relax}} + E_{\text{QP}} \end{aligned} \tag{3}$$

by adding and subtracting the term $E^f_{q-1}(\mathbf{R}_q)$ [11]. (All the formation energies in the above expression as well as throughout the rest of the paper are evaluated with $\mu = E_v$.) This reformulation allows one to combine terms to eliminate most of the DFT errors mentioned above. Figure 1 shows schematically the procedure for calculation of CTLs within the DFT + *GW* formalism. The first bracketed term on the right-hand side of Eq. (3) is a structural relaxation energy E_{relax} (red line in Fig. 1) and the second bracketed term is a QP excitation energy E_{QP} (blue line in Fig. 1). For the excitation energy, one uses the *GW* formalism [6]; while for the relaxation energy, one uses DFT. Since these approaches are proven to give accurate results for the two respective energies, the DFT + *GW* approach ensures an accurate calculation of the appropriate physical quantities and hence the CTL.

The CTL is a thermodynamic quantity and does not depend on the path in the formation energy-generalized coordinate space that one takes to calculate it. In other words, the value of CTL remains unaffected when one adds and subtracts any formation energy to it. In particular, we can alternatively choose to add and subtract $E^f_q(\mathbf{R}_{q-1})$ in Eq. (2). This would correspond to another path (path 2—the green line) in Fig. 1. Path 2 in Fig. 1 is completely independent of the path represented by Eq. (3) (path 1). The QP and relaxation energies involved in the two paths are different. Along path 1, the QP energy required is $E_{q-1}(\mathbf{R}_q) - E_q(\mathbf{R}_q) - E_v$. This can be calculated either as the electron affinity (EA) of the system in charge state q

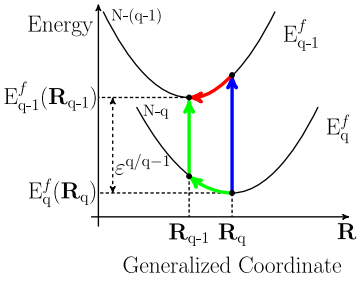

FIG. 1 (color online). Formation energies evaluated with $\mu = E_v$ vs generalized coordinate, illustrating the terms in the DFT + *GW* formalism for the CTL $\varepsilon^{q/q-1}$.

and ionic configuration $\mathbf{R}_q$ or as the ionization potential (IP) of the system in charge state $q - 1$ and ionic configuration $\mathbf{R}_q$. Both calculations would give the same QP energy. However, along path 2 the QP energy required is $E_{q-1}(\mathbf{R}_{q-1}) - E_q(\mathbf{R}_{q-1}) - E_v$. This is different from the QP energy in path 1 and is calculated as the EA (IP) of the system in charge state q $(q - 1)$ and ionic configuration $\mathbf{R}_{q-1}$. The corresponding relaxation energies along the two paths are also different. Calculating the CTL via two independent paths not only serves as a check for our calculations, but also gives an idea about the accuracy of the method. As discussed below, it also reveals that the inclusion of electrostatic corrections (to be discussed) is absolutely necessary to get a reliable CTL.

For the DFT part of our calculation we used an *ab initio* pseudopotential plane-wave method, as implemented in QUANTUM ESPRESSO [12], with PBE [13] exchange correlation functional. We used nonlocal pseudopotentials constructed using the Troullier-Martins [14] scheme with valence configurations $5s^25p^65d^26s^2$ and $2s^22p^4$ for Hf and O, respectively. The electronic wave functions were expanded in plane waves with cutoff energy of 250 Ry. The k-point sampling was restricted to the Γ point in view of the large supercell used. Our calculated lattice parameters for monoclinic hafnia are in excellent agreement with experiment [15] as well as with previous calculations [4]. The QP energies were calculated within the G_0W_0 approximation [6] to the electron self energy as implemented in the BERKELEYGW package [16]. The static dielectric matrix was calculated with a 10 Ry energy cutoff and extended to finite frequencies within the generalized plasmon pole model [6]. The band gap for bulk monoclinic hafnia is calculated to be 6.0 eV, which is in agreement with previous studies 5.45–5.9 [10,17] as well as experiments 5.7–5.9 [18,19].

There are two distinct types of oxygen vacancies (with different coordination) in monoclinic hafnia—threefold coordinated (V_{O_3}) and fourfold coordinated (V_{O_4}). We performed calculations for charge states $q = 0$, 1, 2 for both kind of vacancies, i.e., zero, one, and two missing electrons from the vacancy.

Figure 2(a) shows a schematic of the oxygen vacancy induced QP defect levels in the band gap of hafnia. The defect levels for all the charge states lie deep in the gap. Table I shows our relaxation energies (E_{relax}), QP energies (E_{QP}) and CTLs ($\varepsilon^{q/q-1}$) calculated within our DFT + *GW* approach. Despite the large differences in the QP and relaxation energies used for the calculation in the two paths, the final CTLs via the two paths are within 0.2 eV of one another. This gives us an error estimate of ± 0.1 eV for the calculated CTLs. Along each path, we calculate the QP energy either as EA or IP (of different charge states); while in principle both would give the same QP energy, in practice they could differ by 0.1–0.2 eV.

We emphasize that the QP energies in Table I include an electrostatic correction owing to the supercell geometry

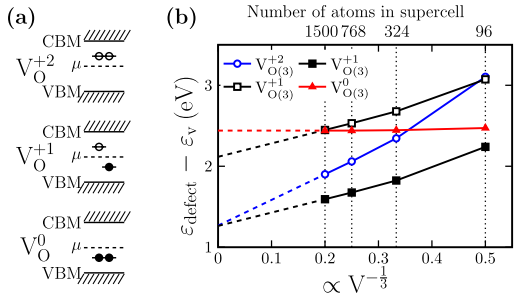

FIG. 2 (color online). (a) Schematic diagram showing oxygen vacancy induced defect levels in the band gap of hafnia for various charge states. (b) Effect of the spurious potential on the defect-state eigenvalues. The plot shows the PBE eigenvalue vs supercell size with respect to the top of the valence band in the same supercell calculation for defect states in V_{O_3} in different charge states. Empty (filled) symbols represent unoccupied (occupied) defect level as per (a).

used, which is an effect neglected in previous DFT + *GW* studies. Within the standard DFT-only methodology (i.e., total energy difference) of calculating CTLs, one may correct the formation energies of charged defects for the unphysical electrostatic terms from the charge on the image defects using Makov-Payne [20] like corrections. Within the DFT + *GW* method, this electrostatic error in the individual DFT eigenvalues in general needs to be accounted for. This is clearly seen in Fig. 2(b): there is a change in the position of the defect levels relative to the valence band maximum as the supercell size is changed. This correction depends on the specific defect state for a given charged defect. The origin of these electrostatic errors in the supercell DFT eigenvalues is the spurious electrostatic potential seen by the electron from charged neighboring defects [21]. Within the standard DFT-only methodology, there is no need to correct each of the eigenvalues (as only total energies are needed), but in the DFT + *GW* method the QP energies are calculated from adding a self energy correction to the DFT eigenvalues and therefore, this spurious interaction term needs to be corrected. To quantify these errors, we plotted the position of the Kohn-Sham defect level with respect to the valence band maximum for various supercell sizes as shown in Fig. 2(b). These calculations were done using the SIESTA code [22] with increasing supercell sizes − the largest of which contained 1499 atoms + the defect. To get the infinite supercell size value, we linearly extrapolated from the largest two supercell sizes. Figure 2(b) shows that the errors are very large and therefore cannot be neglected. The correction along a path depends on the DFT eigenvalue used to calculate the QP energy for that path. For instance, for calculation of $\varepsilon^{+2/+1}$ along one of the paths, the QP energy required is $E_{+2}(\mathbf{R}_{+2}) - E_{+1}(\mathbf{R}_{+2}) - E_v$. This can be calculated as EA (IP) of +2 (+ 1) charged system in which case the DFT eigenvalue of the unoccupied (occupied) defect level of +2 (+ 1) charged system needs to be corrected. The electrostatic correction for occupied and unoccupied defect levels in the +1 charged system is 0.97 eV and unoccupied defect level in the +2 charged system is 1.84 eV. Accounting for these errors is therefore crucial to get a reliable value of CTL.

Our QP defect levels and CTLs strongly disagree with results from previous DFT + *GW* calculations [10]. This disagreement is likely a consequence of their choice of a small supercell and, more importantly, neglect of electrostatic corrections. Ref. [10]'s value of $\varepsilon^{+2/+1}$ for V_{O_3} (V_{O_4}) is 4.00 eV (3.22 eV) and of $\varepsilon^{+1/0}$ is 3.10 eV (2.43 eV); these values are close to our corresponding *uncorrected* values (not shown). Our calculations also strongly disagree with the hybrid functional values [8] of 3.7 eV for $\varepsilon^{+2/+1}$ in V_{O_3} and 4.0 eV for $\varepsilon^{+1/0}$ between $V^{+1}_{O_3}$ and $V^{0}_{O_4}$. Our corresponding values are 2.56 and 3.32 eV, respectively. It is further noted that as expected the Kohn-Sham eigenvalues calculated with hybrid functionals also significantly disagree with our QP energies. Also, in hybrid calculations, even though total energies were corrected for supercell electrostatic errors, the eigenvalues were not. While this is not necessary for the CTL calculated as a total energy difference, it could lead to erroneous results if eigenvalues were used as single-particle excitation energies.

Figure 3 shows the relative formation energy of various charge states for the oxygen vacancies as a function of the electron chemical potential, μ, in monoclinic hafnia based on the values in Table I. The formation energy in Fig. 3 is plotted with respect to the formation energy of $V^0_{O_3}$. The absolute value of the formation energy will depend on the chemical potential of oxygen. As evident from Fig. 3, $V^{+2}_{O_3}$, $V^{+1}_{O_3}$, and $V^0_{O_4}$ are the most stable defects in the system depending on the value of μ. The experimentally relevant CTLs, $\varepsilon^{+2/+1}$ and $\varepsilon^{+1/0}$ would be 2.56 and 3.32 eV from the VBM, respectively. For higher values of the chemical potential, μ, the V_O^{-1}/V_O^{-2} defects may become more stable. Also, shown in Fig. 3 (in shaded grey), is the band gap and the expected band offset for Si (~ 3 eV) at

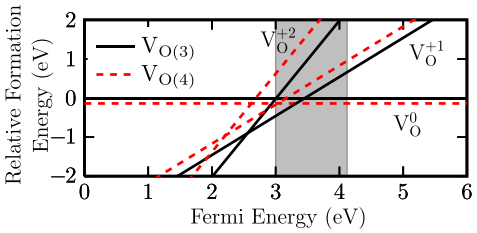

FIG. 3 (color online). Relative formation energy (relative to that of $V^0_{O_3}$) vs chemical potential (or Fermi energy) for charged oxygen vacancies in monoclinic hafnia. The shaded region denotes the placement of the Si band gap at a hafnia-Si interface. The formation energy of $V^0_{O_4}$ is lower than $V^0_{O_3}$ by 0.14 eV.

TABLE I. Table showing the two components contributing to the CTLs for V_{O_3} and V_{O_4} calculated within the DFT + GW methodology. $P1$ ($P2$) refers to Path 1 (2). Row 1 shows the relaxation energy (E_{relax}), row 2 the QP energy (E_{QP}) that includes electrostatic corrections, row 3 the CTL ($\varepsilon^{q/q-1}$) and row 4 the value for $\varepsilon^{q/q-1}$ averaged over both paths. All values are in eV.

	V_{O_3}				V_{O_4}			
	+2/+1		+1/0		+2/+1		+1/0	
	$P1$	$P2$	$P1$	$P2$	$P1$	$P2$	$P1$	$P2$
E_{relax}	−0.64	0.76	−0.57	0.67	−0.75	0.80	−0.55	0.65
E_{QP}	3.30	1.69	3.93	2.88	3.04	1.33	3.46	2.50
$\varepsilon^{q/q-1}$	2.66	2.45	3.36	3.55	2.29	2.13	2.91	3.15
Avg. $\varepsilon^{q/q-1}$	2.56		3.46		2.21		3.03	

the hafnia-Si interface [19]. For p-doped Si next to hafnia, the system is expected to have $V_{O_3}^{+1}$ vacancies.

From Fig. 3, we note that oxygen vacancies are large positive U centers. U is defined as the energy of the reaction: $2V^{+1} \rightarrow V^{2+} + V^{0}$. In terms of the CTLs, U for V^{+1} can be written as

$$\begin{aligned} \mathrm{U} &= E^f_{+2}(\mathbf{R}_{+2}) + E^f_0(\mathbf{R}_0) - 2E^f_{+1}(\mathbf{R}_{+1}) \\ &= -\varepsilon^{+2/+1} + \varepsilon^{+1/0}. \end{aligned} \tag{4}$$

Our calculated values of U for both vacancies ($V_{O_3}^{+1}$ and $V_{O_4}^{+1}$) are given in Table II. Further, U can be broken into two parts—an electronic part (U_{elec}) and a structural relaxation part (U_{relax}) as defined in the curly brackets in Eq. (5) below:

$$\begin{aligned} U &= \{E^f_{+2}(\mathbf{R}_{+1}) + E^f_0(\mathbf{R}_{+1}) - 2E^f_{+1}(\mathbf{R}_{+1})\} \\ &\quad + \{[E^f_{+2}(\mathbf{R}_{+2}) - E^f_{+2}(\mathbf{R}_{+1})] \\ &\quad + [E^f_0(\mathbf{R}_0) - E^f_0(\mathbf{R}_{+1})]\} \\ &\equiv U_{elec} + U_{relax}. \end{aligned} \tag{5}$$

This partitioning of U is instructive because, physically, U_{elec} represents the QP gap of the system in the +1 charge state keeping the structure fixed and U_{relax} represents sum of structural relaxation energies. Physically, $U_{elec} \geq 0$ and $U_{relax} \leq 0$. Table II shows our calculated values of U_{relax} and U_{elec}. The reason for the large relaxation energy is that, in the +1 and +2 charge state, the atoms nearest to the vacancy relax by up to 5%–10% of their bond lengths. This is in agreement with previous studies of relaxation around oxygen vacancies [3,4].

In conclusion, we have reported defect-state QP energies and CTLs of oxygen vacancies in monoclinic hafnia. We find that $V_{O_3}^{+2}$, $V_{O_3}^{+1}$, and $V_{O_4}^{0}$ are the most stable oxygen vacancies in the system as the Fermi level spans the band gap. By calculating the CTLs via two paths in configuration space we gain insight to the charge defect stability and highlighted the importance of electrostatic corrections in supercell defect calculations. Further, we developed an intuitive partitioning of the defect charging energy U into a QP gap and lattice contribution. Contrary to some previous studies, which found negative U or small positive U, the oxygen vacancies are found to be large positive U centers.

TABLE II. U (in eV) for $V_{O_3}^{+1}$ and $V_{O_4}^{+1}$ calculated using the CTLs from Table I. Also shown are the contributions to U from electronic and relaxation components.

	U_{elec}	U_{relax}	U_{total}
$V_{O_3}^{+1}$	2.24	−1.33	0.90
$V_{O_4}^{+1}$	2.13	−1.35	0.81

We thank Alex Demkov for pointing out to us the important role of oxygen vacancies in hafnia and for discussion in the initial stage of this work. We thank Brad Malone, Johannes Lischner, and Georgy Samsonidze for fruitful discussions. This work was supported by National Science Foundation Grant No. DMR10-1006184, the U.S. Department of Energy under Contract No. DE-AC02-05CH11231 and DE-SC0001878. Computational resources have been provided by NSF through TeraGrid resources at NICS. M. J. was supported by the DOE. Part of the simulations were carried out with electronic structure and QP codes developed under NSF support.

[1] G. Ribes *et al.*, IEEE Trans. Device Mater. Reliab. **5**, 5 (2005).
[2] C. Hobbs *et al.*, IEEE Trans. Electron Devices **51**, 971 (2004).
[3] A. S. Foster *et al.*, Phys. Rev. B **65**, 174117 (2002).
[4] J. X. Zheng *et al.*, Phys. Rev. B **75**, 104112 (2007); J. Kang, E.-C. Lee, and K. J. Chang, *ibid.* **68**, 054106 (2003).
[5] P. W. Anderson, Phys. Rev. Lett. **34**, 953 (1975).
[6] M. S. Hybertsen and S. G. Louie, Phys. Rev. B **34**, 5390 (1986).
[7] J. L. Gavartin *et al.*, Appl. Phys. Lett. **89**, 082908 (2006).
[8] P. Broqvist and A. Pasquarello, Appl. Phys. Lett. **89**, 262904 (2006).
[9] K. Xiong *et al.*, Appl. Phys. Lett. **87**, 183505 (2005).
[10] E.-A. Choi and K. J. Chang, Appl. Phys. Lett. **94**, 122901 (2009).

[11] M. Hedström *et al.*, Phys. Rev. Lett. **97**, 226401 (2006); P. Rinke *et al.*, *ibid.* **102**, 026402 (2009).
[12] P. Giannozzi *et al.*, J. Phys. Condens. Matter **21**, 395502 (2009).
[13] J. P. Perdew, K. Burke, and M. Ernzerhof, Phys. Rev. Lett. **77**, 3865 (1996).
[14] N. Troullier and J. L. Martins, Phys. Rev. B **43**, 1993 (1991).
[15] J. Wang, H. P. Li, and R. Stevens, J. Mater. Sci. **27**, 5397 (1992); D. M. Adams *et al.*, J. Phys. Chem. Solids **52**, 1181 (1991); D. W. Stacy, J. K. Johnstone, and D. R. Wilder, J. Am. Ceram. Soc. **55**, 482 (1972).
[16] http://www.berkeleygw.org.
[17] H. Jiang *et al.*, Phys. Rev. B **81**, 085119 (2010); M. Grüning, R. Shaltaf, and G.-M. Rignanese, Phys. Rev. B **81**, 035330 (2010).
[18] S. Sayan *et al.*, J. Appl. Phys. **96**, 7485 (2004).
[19] E. Bersch *et al.*, Phys. Rev. B **78**, 085114 (2008).
[20] G. Makov and M. C. Payne, Phys. Rev. B **51**, 4014 (1995).
[21] S. Lany and A. Zunger, Phys. Rev. B **81**, 113201 (2010); C. Freysoldt *et al.*, Phys. Rev. Lett. **102**, 016402 (2009).
[22] P. Ordejón, E. Artacho, and J. M. Soler, Phys. Rev. B **53**, R10 441 (1996); J. M. Soler *et al.*, J. Phys. Condens. Matter **14**, 2745 (2002).